

Lack of thermodynamic equilibrium in conjugated organic molecular thin films

N. Koch, C. Chan, and A. Kahn

Department of Electrical Engineering, Princeton University, Princeton, New Jersey 08544

J. Schwartz

Department of Chemistry, Princeton University, Princeton, New Jersey 08544

(Received 24 January 2003; published 27 May 2003)

We show that the observation by photoemission spectroscopy of a finite density of occupied states at the Fermi-level on a film of a conjugated organic material (*para*-sexiphenyl) in which alkali metal atoms have been intercalated does not necessarily imply metallicity nor the presence of negative polarons (radical anions). The combination of ultraviolet photoemission spectroscopy and Kelvin probe measurements rules out the presence of surface photovoltage, and reveals that the substrate and the surface of the organic film are not in thermodynamic equilibrium.

DOI: 10.1103/PhysRevB.67.195330

PACS number(s): 73.20.-r, 73.30.+y, 73.61.Ph, 79.60.Fr

I. INTRODUCTION

The physics and chemistry of interfaces between conjugated organic materials (COMs) and inorganic materials, especially metals, have been given particular attention, as virtually every property of such interfaces is crucial to device performance and stability.^{1,2} Ultraviolet photoemission spectroscopy (UPS) is routinely used to obtain information on the electronic structure and energy level alignment at organic/metal interfaces,^{2,3} and the conclusions drawn from these experiments have a considerable impact on our understanding of such interfaces and on the implementation of new strategies towards improved device structures. However, the complexity of electronic and structural processes that take place in molecular materials upon excitations, e.g., relaxation and polarization phenomena in the presence of excess charges, is considerable, and requires the utmost care to ascertain the reliability of conclusions drawn from techniques such as photoemission spectroscopy.

Several groups have reported the presence of a finite density of valence states (DOVS) measured by UPS *at* or even *above* the Fermi level (E_F) following the deposition of small amounts of metal on an organic film.⁴⁻⁸ Whereas pristine organic materials do not have gap states, such states can be introduced by chemical interaction with, or charge transfer from, metal atoms. In particular, alkali and alkaline-earth metal atoms can transfer electrons to unfilled molecular orbitals of the COM. The subsequent structural and electronic changes in the organic molecule lead to gap states usually described in terms of negative polarons (radical anions) and bipolarons (dianions) for nondegenerate ground-state COMs.⁹⁻¹¹ However, the reported presence of filled states *at* or *above* E_F is peculiar and has not been convincingly explained. It has occasionally been attributed to the presence of polarons in the sample (generally at low metal concentrations), and the shift of these states below E_F , which generally occurs at higher metal concentration, has been attributed to the formation of bipolarons.^{4,5} Little attention has been paid to the fact that samples with a DOVS at E_F (at a sufficiently high doping level) should exhibit metallic properties, and that no attempt to elucidate this issue has been made in

these cases. An alternative explanation, put forth by Koch and co-workers,^{12,13} invokes the fact that many COMs, polymer or small molecules, are nearly insulating, wide energy gap materials ($E_g > 2$ eV) with low concentration of defects ($< 10^{15}$ cm⁻³),¹⁴⁻¹⁶ and that thermodynamic equilibrium between substrate and metal-induced surface electronic states may not always be established.

For a pristine molecular film, the alignment of molecular levels with respect to the Fermi level of the substrate is set *at the interface* and the molecular levels are generally *flat throughout the film*,³ at least for film thicknesses smaller than ~ 20 – 50 nm. The deposition of metal atoms induces new gap states, the position of which in the gap is defined by the nature of the metal atom-molecule interaction and by the molecular reorganization. Figure 1(a) shows the schematic energy diagram for the case where the Fermi level represents a meaningful equilibrium across the film. At thermodynamic equilibrium, the upper gap state is below E_F , inducing a shift of all molecular levels with respect to the pristine sample, where the energy levels were flat. The precise shape of the *molecular level bending* inside the film is unknown. It can be straight and slanted, as represented here for a film depleted of charges, or could exhibit a more standard space charge region shape encountered in doped semiconductors. The shape, however, is irrelevant for the present discussion. The hypothetical situation of a lack of thermodynamic equilibrium is illustrated in Fig. 1(b), which, due to the low concentration of free charge carriers in the pristine material, explains the absence of molecular level bending upon metal deposition and the apparently random position of the gap states with respect to the Fermi level of the metal substrate. In the case depicted here, the DOVS from the upper filled gap state overlaps the position of the Fermi level measured from the metal substrate (dotted line).

Alternatively, the absence of thermodynamic equilibrium could result from surface photovoltage (SPV), a phenomenon which has been shown to be significant in photoemission on low doped, wide-gap inorganic semiconductor surfaces and interfaces.¹⁷⁻¹⁹ In SPV, secondary charge carriers generated by the photoemission process in the bulk of the film accumulate near the surface, leading to a steady-state

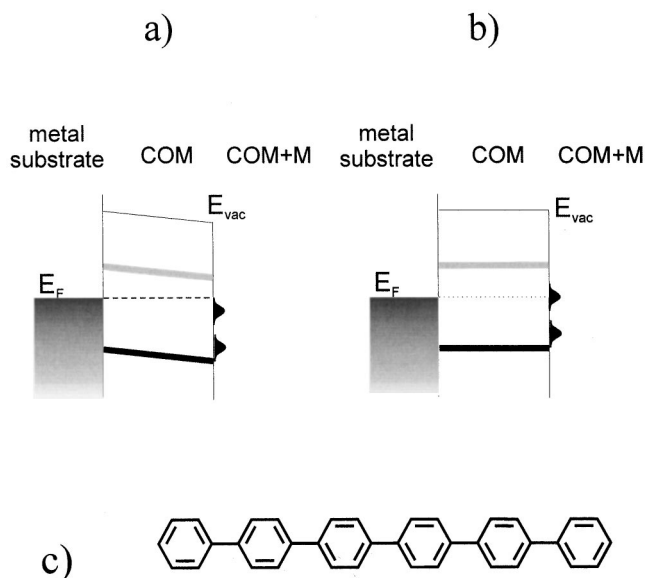


FIG. 1. Schematic energy level diagram for an organic film (COM) on a metallic substrate, showing the HOMO (black bar), the LUMO (gray bar), and metal adatom (M)-induced gap states on the surface: (a) thermodynamic equilibrium, and (b) nonequilibrium. E_{vac} indicates the position of the vacuum level. In (a) the dashed line represents the position of E_F throughout the whole sample in thermodynamic equilibrium. In (b), the dotted line represents the energy position of E_F determined on the metal substrate. (c) chemical structure of $6P$.

electric field which modifies the built-in electric field and shifts all levels to a nonequilibrium position.

To investigate these various possibilities, we carry out here a combined photoemission–Kelvin probe (KP) experiment on an already well studied organic-metal system. The electroluminescent oligomer *para*-sexiphenyl [$6P$, $C_{36}H_{26}$; chemical structure shown in Fig. 1(c)] (Refs. 20 and 21) is chosen as the conjugated organic material because its electronic structure is well understood.^{7,22,23} Furthermore, alkali and alkaline-earth metal atoms intercalated in $6P$ films have been shown to react to give exclusively bipolarons, even at metal/ $6P$ ratios as low as 1% of the saturation concentration.^{12,22,24,25} We investigate the gap states induced by the deposition of cesium, their binding energy with respect to E_F , and the sample work function, with and without ultraviolet radiation. A straightforward conclusion on the presence of DOVS at E_F in photoemission emerges from the comparison of the work functions measured by UPS and KP.

II. EXPERIMENT

Sample preparation, UPS, and KP measurements were made in an ultrahigh vacuum system comprising interconnected preparation and analysis chambers. Thin films of $6P$ were evaporated in the preparation chamber from a resistively heated pinhole-source at a pressure lower than 1×10^{-9} mbar. The substrates consisted of 500-Å films of polycrystalline gold deposited on silicon wafers pre-coated with a thin layer of chromium. The $6P$ thickness was monitored with a quartz microbalance placed next to the substrate.

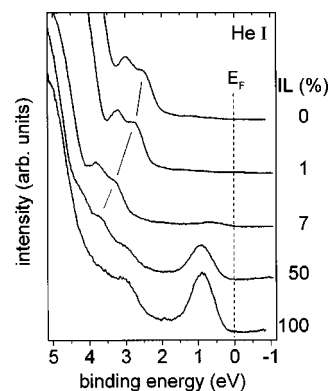


FIG. 2. Low binding energy region of the $6P$ valence spectrum as a function of Cs intercalation level (IL). 100% represents the maximum Cs concentration, i.e., two Cs atoms per $6P$ molecule.

Cs was evaporated from a thoroughly degassed SAES S.p.A. alkali metal dispenser. The pressure remained below 4×10^{-10} mbar during Cs dosing and KP measurements, and below 3×10^{-10} mbar during UPS. KP measurements were performed in complete darkness. UPS was performed with the He I radiation (21.22 eV) of a discharge lamp. The vacuum level of the film was determined from the onset of photoemission with the sample biased negatively at -3 V to clear the work function of the analyzer. The energy resolution in UPS was 120 meV, determined from the width (80–20% intensity) of the gold Fermi-edge. X-ray photoelectron spectroscopy (XPS) with unfiltered Al $K\alpha$ radiation was performed to determine the stoichiometry of samples with maximum intercalation level. The photoelectron cross-section values for $C(1s)$ and $Cs(3d)$ core levels were taken from the literature.²⁶ The photoelectron take-off angle was changed between 15° and 75° in order to investigate possible variance in stoichiometry for different probing depths.²⁷ The samples were kept at room temperature throughout all preparation and measurement steps. We estimate that the experimental error made in the evaluation of the Cs/ $6P$ ratio is $\sim 10\%$.

III. RESULTS AND DISCUSSION

The low binding energy valence spectrum of a 250-Å $6P$ film deposited on Au is displayed as the topmost curve in Fig. 2. The centroids of the highest occupied molecular orbital (HOMO) and HOMO-1 peaks are found at 2.5 and 3.0 eV, respectively. The leading edge of the HOMO peak is at 2.0 eV below the Fermi level of the metal (E_F). From the position of the secondary electron cutoff (not shown here), which gives the position of the vacuum level, we determine the first ionization energy and the work function of the $6P$ film to be 6.1 and 4.1 eV respectively. These values are in very good agreement with published values of the $6P$ ionization energy^{7,23} and of the energy difference between the HOMO and E_F for $6P$ on Au.^{12,28}

Also shown in Figure 2 is the evolution of the spectra of the $6P$ valence orbitals and gap as a function of increasing Cs intercalation level (IL). We define an IL of 100% when further exposure to Cs does not change the photoemission spectrum. Lower ILs are defined with respect to an IL of

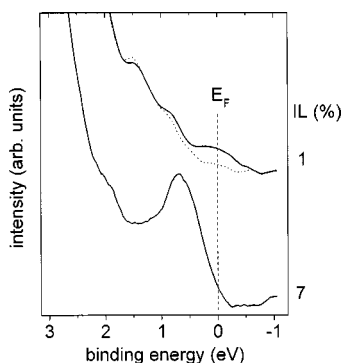


FIG. 3. Close-up of the gap and near E_F region of $6P$ for ILs equal to 1% and 7%, showing the finite DOVS at E_F . The dotted curve represents the spectrum of pristine $6P$, shifted to make up for the work function change.

100%, proportionally to the time of exposure. The analysis of the XPS data (not presented here), using the cross-section mentioned above, show that an IL of 100% corresponds to *two Cs atoms per 6P molecule*, regardless of the photoelectron take-off angle. This shows that, within the depth probed by XPS (~ 20 – 40 Å), the stoichiometry of the sample is homogeneous. The lines in the figure mark the energy shift of the HOMO of still unreacted $6P$ molecules; all other photoemission features corresponding to unreacted $6P$ exhibit the same rigid shift toward higher binding energy. On the intensity scale of Fig. 2, new gap states can be observed for an IL of 7% and upwards. Their binding energy shift follows that of the features of unreacted molecules. For an IL of 100%, the gap states are centered at 3.0 and 0.9 eV below E_F . They are identified as the relaxed HOMO and stabilized filled lowest unoccupied molecular orbital (LUMO), respectively, of $6P$ due to electron transfer from Cs.^{22,24,25} These four ILs are sufficient for the present discussion, as more detailed studies of the same system have been presented elsewhere.^{22,25}

A close-up of the near- E_F energy region of the spectrum for an IL of 1% and 7% is shown in Fig. 3. The dotted curve corresponds to a spectrum from pristine $6P$ shifted in energy to correct for the change in sample work function and align the peaks of unreacted $6P$. The superposition of the two curves shows that the new low binding energy photoemission feature of reacted $6P$ molecules is detectable for an IL of 1%. This feature is *centered* at E_F , leaving a significant fraction of occupied states above E_F . The IL curve of the 7% also shows a finite intensity at E_F (this is a true emission, as instrumental broadening is too small to account for this overlap). Features other than the one at E_F in the upper curve of Fig. 3 stem from photoelectrons excited from deeper valence states by the He 1β satellite photon line (23.09 eV).

Changes in sample work function ($\Delta\phi$) were measured by (i) recording the shift in secondary electron cutoff in UPS,²⁹ and (ii) measuring the contact potential difference between sample and KP tip in complete darkness. These data are plotted in Fig. 4 as a function of the IL. The two measurements are in excellent agreement (within the ~ 0.1 eV experimental error) throughout the range of exposure. The small (≤ 0.1 eV) offset between KP and UPS data for ILs of 1%, 7%, and

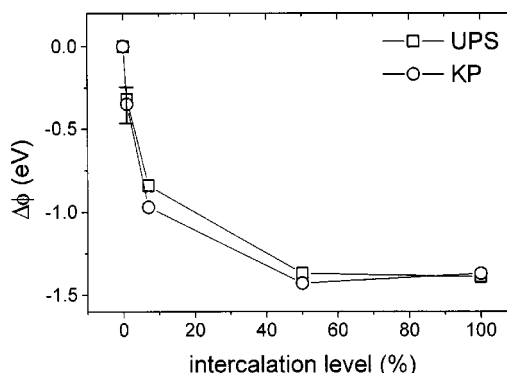


FIG. 4. Change in sample work function ($\Delta\phi$) vs intercalation level measured for Cs-intercalated $6P$ with UPS and KP.

50% is due to the time-delay between the two measurements: Cs diffusion continues on the time scale of our experimental procedure, leading to a continued decrease of sample work function. Additional UPS measurements following the KP measurements yield the same $\Delta\phi$ value as obtained by KP. Thus the error bar in the figure is asymmetrically extended towards a lower work function. The sample work function for an IL of 100% is 2.7 eV.

These experimental results lead to the following interpretation. The stoichiometry of two Cs atoms per $6P$ molecule at an IL of 100% is consistent with the fact that Cs intercalation leads to negative bipolarons of $6P$ only. The analysis of the two new gap states (relaxed HOMO and filled, stabilized LUMO) at a low IL reveals no change in their lineshape or energy position relative to each other and relative to energy levels from unreacted $6P$ as a function of the IL (also see Refs. 7, 12 and 25). Thus, the gap states originate from the same species, i.e., bipolaron, throughout the full deposition sequence, as the negative polaron would be expected to have a different relative binding energy.³⁰ Note also that solid-state cyclo-voltammetry experiments on $6P$ show that the first reduction is due to a two-electron transfer, indicating the immediate formation of dianions (bipolarons).³¹

Furthermore, it has been shown that the presence of a DOVS at E_F for alkali metal- or Ca-intercalated $6P$ films depends directly on the organic film thickness and on the initial work function of the substrate. The experimental findings of three separate studies are schematically depicted in Fig. 5 as a summary of energy positions of the metal-induced low binding energy gap state relative to E_F measured at low

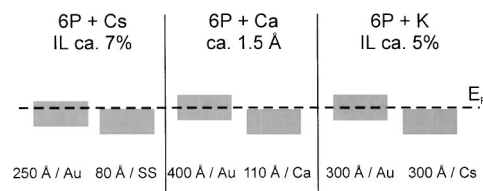


FIG. 5. Schematic energy level diagram of the low binding energy gap state (induced by the charge transfer from metal atoms) for $6P$ films at low ILs of Cs (left), Ca (middle), and K (right). The $6P$ thickness and the substrate (SS...stainless steel) are noted below the respective examples.

TABLE I. Summary of presence of gap states at E_F for alkali metal intercalated $6P$ films as a function of film thickness and substrate work function

Organic film	Substrate ϕ	DOVS as E_F
thick	high	yes
thick	low	no
thin	high	no
thin	low	no

ILs. The left part of the figure shows that the Cs-induced DOVS in the $6P$ gap is *below* E_F when the thickness of the organic film is $\leq 80 \text{ \AA}$,²⁵ whereas it is *at* E_F in the present case with a $6P$ thickness of 250 \AA . The middle part illustrates the case of calcium (Ca) on $6P$, where states *at* E_F are measured when a *large work function* substrate like Au is used, which raises the pristine $6P$ levels relative to the Fermi level of the metal and gives a pristine $6P$ work function of 4.2 eV . On the other hand, the states are *below* E_F when a *low work function* substrate like Ca is used, which lowers the pristine $6P$ levels relative to the Fermi level of the metal and gives a pristine $6P$ work function of 3.4 eV .¹² Finally, the right hand part summarizes the case of potassium (K) on $6P$. This case is similar to the one described for Ca, but the $6P$ films are of comparable thickness ($\sim 300 \text{ \AA}$) for the high and low work function substrates (Au and Cs, respectively). In line with the abovementioned results, the K-induced DOVS is found *below* E_F for the low work function substrate Cs, and *at* E_F for the high work function Au substrate.³² Thus, for thin organic films, or when the work function of the pristine organic film is small, no DOVS is observed at or above E_F at any given IL, confirming that bipolarons only are formed in the organic film. A summary of the observations discussed above is given in Table I. In the case of $6P$, the transition between “thick” and “thin” films would be around 200 \AA .

Having ruled out the presence of Cs-induced polarons and demonstrated that organic film thickness and initial work function play a crucial role in the position of the DOVS, we now turn to surface photovoltage (SPV) as a possible mechanism for the appearance of DOVSs at E_F . Under the SPV scenario, nonequilibrium is the result of sample illumination,

and occupied electronic levels *in the dark* should be below E_F even for the smallest amount of bipolarons present on the sample surface. In order to test for SPV, we measured the sample work function change as a function of Cs exposure with KP in complete darkness. As is clear from Fig. 4, the work function changes measured by UPS and KP are in excellent agreement. This result rules out the occurrence of ultraviolet light-induced surface photovoltage in this particular case, and leads to the conclusion that the low coverage Cs-induced gap states *are* indeed found at an energy equal to or above the Fermi level of the substrate [as depicted in Fig. 1(a)]. Consequently, the sample surface (with bipolarons present) and the substrate are not in thermodynamic equilibrium at low ILs.

As the total exposure to Cs increases, metal atoms diffuse through the film and react to form bipolarons in the bulk. The effective thickness of pristine $6P$ is reduced and thermodynamic equilibrium is slowly established, as shown by the progressive change of the *measured* work function of the organic film. The dependence of the presence of a metal-induced DOVS at E_F on the organic film thickness, and the importance of diffusion of the metal atoms is fully supported by the results of Fig. 5. For the present $6P$ thickness, Cs has presumably diffused through the whole $6P$ film for an IL between 7% and 50%. Yet, detailed mechanisms leading to the gradual decrease of the sample work function, such as the reduction of the substrate work function by Cs diffusing to the interface, cannot be ascertained from the present experiments alone, and will be the subject of future investigations.

IV. SUMMARY

We have shown that thermodynamic equilibrium between the substrate and the surface of a thin molecular film cannot be implicitly assumed. Wide gap conjugated materials may act as electrical insulators, precluding the alignment of E_F throughout the film and leading to misinterpretations of photoemission data of organic/inorganic interfaces.

Support of this work by the NSF (DMR-0097133) and by the New Jersey Center for Optoelectronics is gratefully acknowledged. We would like to thank Professor J.-J. Pireaux for detailed discussions.

¹ *Handbook of Conducting Polymers*, 2nd ed., edited by T. Skotheim, R. Elsenbaumer, and J. Reynolds (Dekker, New York, 1997).

² *Conjugated Polymer and Molecular Interfaces: Science and Technology for Photonic and Optoelectronic Applications*, edited by W. R. Salaneck, K. Seki, A. Kahn, and J.-J. Pireaux (Dekker, New York, 2001).

³ H. Ishii, K. Sugiyama, E. Ito, and K. Seki, *Adv. Mater. (Weinheim, Ger.)* **11**, 605 (1999).

⁴ G. Iucci, K. Xing, M. Lögdlund, M. Fahlman, and W. R. Salaneck, *Chem. Phys. Lett.* **244**, 139 (1995).

⁵ G. Greczynski, M. Fahlman, and W. R. Salaneck, *J. Chem. Phys.* **113**, 2407 (2000).

⁶ N. Koch, H. Oji, E. Ito, E. Zojer, H. Ishii, G. Leising, and K. Seki, *Appl. Surf. Sci.* **175**, 764 (2001).

⁷ N. Koch, A. Rajagopal, G. Leising, and J.-J. Pireaux, in *Conjugated Polymer and Molecular Interfaces: Science and Technology for Photonic and Optoelectronic Applications* (Ref. 2), p. 205.

⁸ G. Greczynski, M. Fahlman, W. R. Salaneck, N. Johansson, D. A. d. Santos, A. Dkhissi, and J. L. Brédas, *J. Chem. Phys.* **116**, 1700 (2002).

⁹ M. Pope and C. E. Swenberg, *Electronic Processes in Organic Crystals and Polymers* (Oxford University Press, Oxford, 1999).

¹⁰ E. M. Conwell and H. A. Mizes, *Phys. Rev. B* **44**, 937 (1991).

¹¹ D. Baeriswyl, D. K. Campbell, and S. Mazumdar, in *Conjugated*

- Conducting Polymers*, edited by H. Kiess (Springer, New York, 1992), Vol. 102.
- ¹²N. Koch, A. Rajagopal, J. Ghijsen, R. L. Johnson, G. Leising, and J. J. Pireaux, *J. Phys. Chem. B* **104**, 1434 (2000).
- ¹³N. Koch, E. Zojer, A. Rajagopal, J. Ghijsen, R. L. Johnson, G. Leising, and J. J. Pireaux, *Adv. Funct. Mater.* **11**, 51 (2001).
- ¹⁴S. Möller and G. Weiser, *Chem. Phys.* **246**, 483 (1999).
- ¹⁵E. J. W. List, C. H. Kim, J. Shinar, A. Pogantsch, K. Petritsch, G. Leising, and W. Graupner, *Synth. Met.* **116**, 81 (2001).
- ¹⁶N. Hayashi, H. Ishii, Y. Ouchi, and K. Seki, *J. Appl. Phys.* **92**, 3784 (2002).
- ¹⁷M. H. Hecht, *J. Vac. Sci. Technol. B* **8**, 1018 (1990).
- ¹⁸M. Alonso, R. Cimino, and K. Horn, *Phys. Rev. Lett.* **64**, 1947 (1990).
- ¹⁹D. Mao, A. Kahn, M. Marsi, and G. Margaritondo, *Phys. Rev. B* **42**, 3228 (1990).
- ²⁰M. Era, T. Tsutsui, and S. Saito, *Appl. Phys. Lett.* **67**, 2436 (1995).
- ²¹S. Tasch, C. Brandstatter, F. Meghdadi, G. Leising, G. Froyer, and L. Athouel, *Adv. Mater. (Weinheim, Ger.)* **9**, 33 (1997).
- ²²M. G. Ramsey, M. Schatzmayr, S. Stafstrom, and F. P. Netzer, *Europhys. Lett.* **28**, 85 (1994).
- ²³S. Narioka, H. Ishii, K. Edamatsu, K. Kamiya, S. Hasegawa, T. Ohta, N. Ueno, and K. Seki, *Phys. Rev. B* **52**, 2362 (1995).
- ²⁴M. G. Ramsey, D. Steinmuller, and F. P. Netzer, *Phys. Rev. B* **42**, 5902 (1990).
- ²⁵N. Koch, G. Leising, L. M. Yu, A. Rajagopal, J. J. Pireaux, and R. L. Johnson, *J. Vac. Sci. Technol. A* **18**, 295 (2000).
- ²⁶J. J. Yeh and I. Lindau, *At. Data Nucl. Data Tables* **32**, 1 (1985).
- ²⁷C. D. Wagner, W. M. Riggs, L. E. Davis, J. F. Moulder, and G. E. Muilenberg, *Handbook of X-ray photoelectron spectroscopy* (Perkin-Elmer, Eden Prairie, MN, 1978).
- ²⁸H. Oji, E. Ito, M. Furuta, K. Kajikawa, H. Ishii, Y. Ouchi, and K. Seki, *J. Electron Spectrosc. Relat. Phenom.* **101–103**, 517 (1999).
- ²⁹A. Rajagopal and A. Kahn, *J. Appl. Phys.* **84**, 355 (1998).
- ³⁰D. Steinmüller, M. G. Ramsey, and F. P. Netzer, *Phys. Rev. B* **47**, 13 323 (1993).
- ³¹K. Meerholz and J. Heinze, *Angew. Chem., Int. Ed. Engl.* **29**, 692 (1990).
- ³²N. Koch, M. Grioni, J.-J. Pireaux, H. Oji, H. Ishii, and K. Seki (unpublished).